

Station-Keeping on Near-Rectilinear Halo Orbits via Full-State Targeting Model Predictive Control

Shimane, Yuri; Di Cairano, Stefano; Ho, Koki; Weiss, Avishai

TR2025-100 July 09, 2025

Abstract

We develop a model predictive control (MPC) policy for station-keeping (SK) on a Near-Rectilinear Halo Orbit (NRHO). Leveraging the controllability obtained from a control horizon consisting of two maneuvers, the proposed MPC policy achieves full-state tracking of a reference NRHO. By spacing the maneuvers one revolution apart, our method abides by the typical mission requirement that at most one maneuver is utilized for SK during each NRHO revolution. Through full-state tracking, the proposed policy does not suffer from phase deviation in the along-track direction of the reference NRHO, a common drawback of existing SK methods with a single maneuver per revolution. Numerical simulations demonstrate that the proposed approach successfully maintains the spacecraft's motion both in space and phase along the NRHO, with tighter tracking than state-of-the-art SK methods and comparable delta-V performance.

American Control Conference (ACC) 2025

© 2025 MERL. This work may not be copied or reproduced in whole or in part for any commercial purpose. Permission to copy in whole or in part without payment of fee is granted for nonprofit educational and research purposes provided that all such whole or partial copies include the following: a notice that such copying is by permission of Mitsubishi Electric Research Laboratories, Inc.; an acknowledgment of the authors and individual contributions to the work; and all applicable portions of the copyright notice. Copying, reproduction, or republishing for any other purpose shall require a license with payment of fee to Mitsubishi Electric Research Laboratories, Inc. All rights reserved.

Station-Keeping on Near-Rectilinear Halo Orbits via Full-State Targeting Model Predictive Control

Yuri Shimane¹, Stefano Di Cairano², Koki Ho³, and Avishai Weiss⁴

Abstract—We develop a model predictive control (MPC) policy for station-keeping (SK) on a Near-Rectilinear Halo Orbit (NRHO). Leveraging the controllability obtained from a control horizon consisting of two maneuvers, the proposed MPC policy achieves full-state tracking of a reference NRHO. By spacing the maneuvers one revolution apart, our method abides by the typical mission requirement that at most one maneuver is utilized for SK during each NRHO revolution. Through full-state tracking, the proposed policy does not suffer from phase deviation in the along-track direction of the reference NRHO, a common drawback of existing SK methods with a single maneuver per revolution. Numerical simulations demonstrate that the proposed approach successfully maintains the spacecraft’s motion both in space and phase along the NRHO, with tighter tracking than state-of-the-art SK methods and comparable delta-V performance.

I. INTRODUCTION

Libration point orbits (LPOs) are expected to play a central role in upcoming lunar exploration. Most notably, the Lunar Gateway will be placed into the 9:2 resonant southern Near-Rectilinear Halo Orbit (NRHO) about the Earth-Moon L2 point [1]. Due to the instability of LPOs, station-keeping (SK) maneuvers are required. SK involves maintaining the spacecraft in the vicinity of a pre-computed reference NRHO, or *baseline*, despite estimation error, modeling error, and control execution error. To date, few missions have flown on LPOs, and thus SK techniques for LPOs are still active areas of research.

In LPO missions, SK maneuvers should be as infrequent as possible in order to allocate time for other activities, such as operating the mission’s payloads, or communicating with ground stations on Earth. In the case of the NRHO, a typical mission requirement is that, at most, a single SK maneuver per revolution about the Moon be conducted. One popular approach that adheres to this requirement is *x-axis crossing control* [2], [3], which employs a shooting method to design the corrective maneuver. In *x-axis crossing control*, a single 3-degrees-of-freedom (DOF) control maneuver is applied once every revolution such that a subset of the spacecraft state at perilune tracks the baseline. Both the recent CAPSTONE mission [4] and the upcoming Gateway [2] use variants of *x-axis crossing control*.

One challenge with *x-axis crossing control* is that at most three state components can be assigned. In spite of the lower DOF than the order of the system, *x-axis crossing control* maintains the spacecraft near the baseline by leveraging the NRHO’s plane of symmetry: a subset of the predicted spacecraft state at the intersection with this plane of symmetry is matched to the corresponding subset of the baseline at its intersection with the same plane. Due to the use of the plane of symmetry, there exists a discrepancy between the epoch in which the spacecraft state crosses the plane and the epoch in which the baseline crosses the plane. The mismatch in epoch causes the steered path to experience a phase angle disparity, where the spacecraft’s position along the orbit drifts ahead or behind the baseline. Over a long mission duration, the phase disparity risks unexpected communication blackouts and/or eclipses. To date, the phase disparity has been treated by ad-hoc heuristics, e.g. augmenting the targeting scheme with the epoch at which the symmetry event occurs [2], [5], [6], or replacing the targeting scheme by a constrained optimization problem formulation [7]. For further details, see [8] and references therein.

We propose a model predictive control (MPC) policy that overcomes the phase disparity via full-state targeting. By considering two maneuvers spaced one revolution apart within the MPC’s control horizon, sufficient controllability is recovered to track all 6 state components. Meanwhile, the maneuvers’ one-revolution spacing ensures that our approach remains consistent with the requirement of using only one maneuver per revolution along the NRHO. An economic objective [9] based solely on the maneuver cost is adopted to ensure the SK cost is minimized. The proposed MPC, hereafter denoted as SKMPC, consists of sequentially solving a second-order cone program (SOCP) that steers the state of the spacecraft to the vicinity of the baseline at the end of its targeting horizon; the SOCP is re-instantiated by linearizing the dynamics about the steered state from the previous iteration until the final state propagated with nonlinear dynamics lies sufficiently close to the baseline. We briefly discuss the recursive feasibility of the proposed MPC policy and numerically demonstrate that its performance is comparable to other, ad-hoc approaches such as the *x-axis crossing control* scheme. Other control theoretic, MPC-based approaches [10]–[13] also adopt a full-state tracking approach, however they do not account for the realistic single maneuver per revolution requirement considered in this work.

The remainder of this paper is organized as follows. In Section II, we introduce the spacecraft dynamics model, LPOs, and discuss NRHO stability. Section III develops the

^{1,3}Y. Shimane and K. Ho are with the Daniel Guggenheim School of Aerospace Engineering, Georgia Institute of Technology, Atlanta, GA 30332, USA Emails: {yuri.shimane, kokiho} at gatech.edu

^{2,4}S. Di Cairano and A. Weiss are with Mitsubishi Electric Research Laboratories (MERL), Cambridge, MA 02139, USA Emails: {dicairano, weiss} at merl.com

MPC policy for SK on NRHOs. Section IV outlines the numerical experiment setup for demonstrating the proposed algorithm, and results are provided in Section V. Finally, we provide concluding remarks in Section VI.

II. BACKGROUND

A. Spacecraft Dynamics Model

The spacecraft's motion is modeled in the inertial frame \mathcal{F}_{Inr} , centered at the Moon. The state of the spacecraft $\mathbf{x} \in \mathbb{R}^6$ consists of the Cartesian position $\mathbf{r} \in \mathbb{R}^3$ with respect to the Moon, along with the rate of change of \mathbf{r} in \mathcal{F}_{Inr} , denoted as $\mathbf{v} \in \mathbb{R}^3$. The equations of motion are given by [14]

$$\dot{\mathbf{x}} = \mathbf{f}[\mathbf{x}(t), t] = \begin{bmatrix} \mathbf{v} \\ -\frac{\mu}{r^3}\mathbf{r} + \mathbf{a}_{\text{J2}} + \sum_i \mathbf{a}_{N_i} + \mathbf{a}_{\text{SRP}} \end{bmatrix}, \quad (1)$$

where $r = \|\mathbf{r}\|_2$, and μ is the gravitational parameter of the Moon. The derivative of \mathbf{v} consists, in order, of the Keplerian acceleration due to the Moon, J2 perturbation of the Moon \mathbf{a}_{J2} , gravitational perturbations by other celestial bodies \mathbf{a}_{N_i} , and the solar radiation pressure (SRP) \mathbf{a}_{SRP} . These terms are given, respectively, by

$$\begin{aligned} \mathbf{a}_{\text{J2}} &= \mathbf{T}_{\text{Inr}}^{\text{PA}} \left(-\frac{3\mu J_2 R_{\text{Moon}}^2}{2r^5} \begin{bmatrix} (1 - 5(z_{\text{PA}}/r)^2) x_{\text{PA}} \\ (1 - 5(z_{\text{PA}}/r)^2) y_{\text{PA}} \\ (3 - 5(z_{\text{PA}}/r)^2) z_{\text{PA}} \end{bmatrix} \right), \\ \mathbf{a}_{N_i} &= -\mu_i \left(\frac{\mathbf{r}_i}{r_i^3} + \frac{\mathbf{d}_i}{d_i^3} \right), \\ \mathbf{a}_{\text{SRP}} &= P_{\text{Sun}} \left(\frac{\|\mathbf{d}_{\text{Earth}} - \mathbf{d}_{\text{Sun}}\|_2}{r_{\text{Sun}}} \right)^2 \frac{C_r A}{m} \frac{\mathbf{r}_{\text{Sun}}}{r_{\text{Sun}}}, \end{aligned}$$

where J_2 is the coefficient due to the oblateness of the Moon, R_{Moon} is the equatorial radius of the Moon, where $[x_{\text{PA}}, y_{\text{PA}}, z_{\text{PA}}]$ is the position vector components of the spacecraft resolved in the Moon's principal axes frame \mathcal{F}_{PA} , $\mathbf{T}_{\text{Inr}}^{\text{PA}} \in \mathbb{R}^{3 \times 3}$ is the transformation matrix from \mathcal{F}_{PA} to \mathcal{F}_{Inr} , μ_i is the gravitational parameter of body i , \mathbf{d}_i is the position of body i with respect to the Moon, $d_i = \|\mathbf{d}_i\|_2$, $\mathbf{r}_i = \mathbf{r} - \mathbf{d}_i$ is the position of the spacecraft with respect to body i in \mathcal{F}_{Inr} , $r_i = \|\mathbf{r}_i\|_2$, P_{Sun} is the SRP magnitude at the 1 astronomical unit, C_r is the radiation pressure coefficient, and A/m is the pressure area-to-mass ratio of the spacecraft. In this work, third-body perturbations of the Earth and the Sun are included. Note that \mathbf{a}_{N_i} and \mathbf{a}_{SRP} in equation (1) are time-dependent, making \mathbf{f} non-autonomous. Constants in the equations of motion and ephemerides of celestial bodies are taken from the SPICE toolkit [15].

An initial linear perturbation $\delta\mathbf{x}(t_0)$ can be linearly mapped to time t , denoted as $\delta\mathbf{x}(t)$, via the state-transition matrix (STM) $\Phi(t, t_0) \in \mathbb{R}^6$ by

$$\delta\mathbf{x}(t) = \Phi(t, t_0)\delta\mathbf{x}(t_0). \quad (2)$$

The Jacobian of the dynamics may be used to construct the STM by solving the matrix initial value problem (IVP)

$$\begin{aligned} \dot{\Phi}(t, t_0) &= \frac{\partial \mathbf{f}(\mathbf{x}, t)}{\partial \mathbf{x}} \Phi(t, t_0), \\ \Phi(t_0, t_0) &= \mathbf{I}_n. \end{aligned} \quad (3)$$

In the remainder of this work, the shorthand notations $\mathbf{x}_j = \mathbf{x}(t_j)$ and $\Phi_{j,i} = \Phi(t_j, t_i)$ are used. For ease of notation, we express the four 3-by-3 block submatrices of $\Phi_{j,i}$ as

$$\Phi_{j,i} = \begin{bmatrix} \Phi_{j,i}^{rr} & \Phi_{j,i}^{rv} \\ \Phi_{j,i}^{vr} & \Phi_{j,i}^{vv} \end{bmatrix}. \quad (4)$$

Assuming impulsive thrusts are available to control the spacecraft state and are of much smaller magnitude compared to the dominant forces, we can approximate the impact of a control action at time t_k mapped to time t_{k+1} by

$$\mathbf{x}_{k+1} = \mathbf{x}_k + \int_{t_k}^{t_{k+1}} \mathbf{f}[\mathbf{x}(t), t] dt + \begin{bmatrix} \Phi_{k+1,k}^{rv} \\ \Phi_{k+1,k}^{vv} \end{bmatrix} \mathbf{u}_k, \quad (5)$$

where $\mathbf{u}_k \in \mathbb{R}^3$ is an impulsive change in velocity.

B. Canonical Scales

There is a large discrepancy in orders of magnitude between \mathbf{r} components expressed in km and \mathbf{v} components expressed in km/s, which causes the STM to have poor numerical conditioning. As a countermeasure, the dynamics from equation (1) can be resolved in terms of canonical scales, where \mathbf{r} is in terms of some length unit LU, and \mathbf{v} is in terms of some velocity unit VU. In this work, we begin by choosing an appropriate value of LU, then define $\text{VU} \triangleq \sqrt{\mu/\text{LU}}$. The canonical time unit TU simply follows as $\text{TU} = \text{LU}/\text{VU}$. Once LU, TU, and VU are defined, all dynamical coefficients appearing in equation (1) may be re-scaled accordingly.

The appropriate choice of LU is investigated by looking at the condition number κ of the N revolution STM $\Phi_{t_0+N\Delta T, t_0}$ along the NRHO starting at an arbitrarily chosen initial state, $\kappa(\Phi_{t_0+\Delta T, t_0}) \triangleq \|\Phi_{t_0+\Delta T, t_0}\|_2 \|\Phi_{t_0+\Delta T, t_0}^{-1}\|_2$, where ΔT is the approximate period of the NRHO. For each LU sampled from a range of values between 1000 km and 200 000 km, $\Phi_{t_0+N\Delta T, t_0}$ is constructed by integrating the canonically scaled matrix IVP (3). Figure 1 shows the variation of κ against LU for N between 1 and 7 revolutions. In this work, to have an easily interpretable value that also results in reasonable κ , LU = 100 000 km is selected.

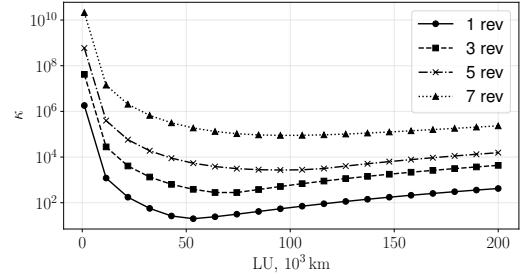


Fig. 1: STM condition number against canonical length unit

C. Libration Point Orbits

Libration point orbits (LPOs) refer to bounded motions that revolve around libration points of three-body systems, such as the Earth-Moon-spacecraft system. While periodic

LPOs can only exist in simplified dynamics models such as restricted three-body problems, quasi-periodic motion still exists in the full-ephemeris dynamics model (1) adopted in this work. LPOs offer mission designers an attractive alternative to “traditional” orbital motions revolving around planetary bodies as they cover a different spatial region and at various energy levels. For example, the southern NRHO about the Earth-Moon L2 has been selected as the location for the Lunar Gateway, a planned crew station in cislunar space [16]. We use the 15-year-long baseline NRHO generated by NASA [1] in the full-ephemeris dynamics.

D. Stability on Near Rectilinear Halo Orbit

Many LPOs, including the NRHO, possess both stable and unstable subspaces. The existence of the unstable subspace on LPOs necessitates SK activities in order to prevent the spacecraft from diverging away from the baseline quasi-periodic path in an inherently uncertain environment. We introduce the *osculating true anomaly* θ , which follows the traditional Keplerian definition for a spacecraft orbiting the Moon, given by $\theta(t) = \text{atan2}(hv_r, h^2/r - \mu)$, where $h = \|\mathbf{h}\|_2 = \|\mathbf{r} \times \mathbf{v}\|_2$ is the angular momentum, and $v_r = \mathbf{r} \cdot \mathbf{v}/r$ is the radial velocity. It is known that the dynamics is most sensitive at *perilune* where $\theta = 0^\circ$, where the spacecraft is closest to the origin, and least sensitive at *apolune* where $\theta = 180^\circ$ [16]. For further details on the dynamics of the NRHO, see [16] and references therein.

SK maneuvers are typically placed around apolune where the dynamics are less sensitive, making the SK activity more robust to navigation and control execution errors [3]. In this work, in accordance with operational plans for the Gateway [2], controls are assumed to have to occur at an osculating true anomaly of 200° , denoted hereafter as the *maneuver true anomaly* θ_{man} . We also choose to target the baseline at an apolune N revolutions in the future to minimize the targeting sensitivity as well. In summary, the controller in this work aims to design an SK maneuver at θ_{man} to steer the state near the baseline at the N^{th} apolune into the future, approximately N revolutions later.

Further information on the deformation of the flow at time t given an initial perturbation $\delta\mathbf{x}(t_0)$ can be quantified by taking the Euclidean norm of (2), $\|\delta\mathbf{x}(t)\|_2^2 = \delta\mathbf{x}(t_0)^T \mathbf{G} \delta\mathbf{x}(t_0)$, where $\mathbf{G} \triangleq \Phi_{t,t_0}^T \Phi_{t,t_0} \in \mathbb{R}^{6 \times 6}$ is the right Cauchy Green Tensor (CGT) [17]. The eigenvectors of \mathbf{G} are denoted as \mathbf{y}_i , where $\sigma_i \mathbf{G} = \mathbf{G} \mathbf{y}_i$ and \mathbf{y}_i^s denote the stable eigenvectors. These vectors will be used in Section III-B.2 to form a terminal set constraint.

III. FULL-STATE TARGETING MPC FOR STATION-KEEPING ON NRHO

A. Problem Formulation

Let \mathcal{U} denote the admissible control set, N denote the number of revolutions until the targeted apolune along the baseline, which occurs at some future time t_N , and $\mathcal{X}(t_N)$ denote the terminal constraint set at time t_N . The control horizon consists of $2 \leq K \leq N$ impulsive maneuvers, denoted as $\mathbf{u}_k \in \mathbb{R}^3$ for $k = 0, \dots, K-1$. These maneuvers

are placed at the K earliest instances in time where $\theta(t) = \theta_{\text{man}}$ occurring between times t_{invoked} , when the controller is invoked, and t_N . A maneuver time t_k for $k = 0, \dots, K-1$ thus satisfies the condition

$$\theta(t_k) = \theta_{\text{man}}, \quad t_k \geq t_{\text{invoked}} + k\Delta T. \quad (6)$$

We hereafter assume without loss of generality that the controller is invoked when $\theta(t_{\text{invoked}}) = \theta_{\text{man}}$, such that $t_0 = t_{\text{invoked}}$. These maneuvers are designed to steer the current state to be in $\mathcal{X}(t_N)$. A minimization problem is formulated with an economic sum-of-2-norm objective of the K maneuvers, which corresponds directly to the propellant mass consumed via Tsiolkovsky’s rocket equation [14]. The finite-horizon discrete-time optimal control problem of the SKMPC is given by

$$\min_{\mathbf{u}_0, \dots, \mathbf{u}_{K-1}} \sum_{k=0}^{K-1} \|\mathbf{u}_k\|_2 \quad (7a)$$

$$\text{s.t. } \mathbf{x}_0^N + \sum_{k=0}^{K-1} \begin{bmatrix} \Phi_{N,k}^{rv} \\ \Phi_{N,k}^{vv} \end{bmatrix} \mathbf{u}_k \in \mathcal{X}(t_N), \quad (7b)$$

$$\mathbf{u}_k \in \mathcal{U}, \quad \forall k = 0, \dots, K-1. \quad (7c)$$

where $\mathbf{x}_0^N \triangleq \text{vec}(\mathbf{r}_0^N, \mathbf{v}_0^N)$ denote the initial state propagated until the end of the prediction horizon, where

$$\mathbf{x}_0^N = \begin{bmatrix} \mathbf{r}_0^N \\ \mathbf{v}_0^N \end{bmatrix} = \mathbf{x}(t_0) + \int_{t_0}^{t_N} \mathbf{f}[\mathbf{x}(t), t] dt. \quad (8)$$

The STM submatrices $\Phi_{N,k}^{rv}$ and $\Phi_{N,k}^{vv}$ are constructed by linearizing the nonlinear flow about the integration in equation (8). The use of the linearized dynamics in (7b) implicitly assumes that the control actions \mathbf{u}_k shifts the state within some trust-region $\delta \in \mathbb{R}^6$, such that $\|\mathbf{x}_0^N - \mathbf{F}_{\mathbf{u}}[\mathbf{x}(t), \mathbf{u}_0, \dots, \mathbf{u}_{K-1}, t]\| \leq \delta$, where $\mathbf{F}_{\mathbf{u}}$ is the dynamics \mathbf{f} piece-wise integrated, with impulsive controls applied at times t_0, \dots, t_{K-1} , and the inequality applies element-wise.

For the admissible control set \mathcal{U} , we consider the set of all controls with magnitudes upper-bounded by a maximum executable control magnitude u_{max} ,

$$\mathcal{U} = \{\mathbf{u} \in \mathbb{R}^3 : \|\mathbf{u}\|_2 \leq u_{\text{max}}\}. \quad (9)$$

B. Definition of Terminal Constraint Set

A straightforward choice to remain in the vicinity of the baseline is to consider an ellipsoidal $\mathcal{X}(t_N)$. As will be demonstrated later, an ellipsoidal $\mathcal{X}(t_N)$ yields performances that are comparable to other state-of-the-art schemes such as x -axis control. In addition, we also consider an alternative $\mathcal{X}(t_N)$ based on the NRHO’s stable subspace to evaluate the extent to which the information of stable directions in the dynamics can improve the SKMPC’s performance.

1) *Ellipsoid*: A simple terminal constraint set can be defined by a 6D ellipsoid centered at the baseline state at time t_N , denoted as $\mathbf{x}_{N,\text{ref}} \triangleq [\mathbf{r}_{N,\text{ref}}^T, \mathbf{v}_{N,\text{ref}}^T]^T$, with radii ϵ_r in position components and ϵ_v in velocity components. The corresponding set $\mathcal{X}_{\text{ell}}(t_N)$ is given by

$$\mathcal{X}_{\text{ell}}(t_N) = \{\mathbf{x} \in \mathbb{R}^n : \|\mathbf{r} - \mathbf{r}_{N,\text{ref}}\|_2 \leq \epsilon_r, \|\mathbf{v} - \mathbf{v}_{N,\text{ref}}\|_2 \leq \epsilon_v\}, \quad (10)$$

where ϵ_r and ϵ_v determine the magnitude of the apses of the ellipsoid, and serve as tuning parameters. The terminal constraint (7b) can be replaced by two second-order cone (SOC) constraints, given by

$$\left\| \sum_{k=0}^{K-1} \Phi_{N,k}^{rv} \mathbf{u}_k + \mathbf{r}_0^N - \mathbf{r}_{N,\text{ref}} \right\|_2 \leq \epsilon_r, \quad (11a)$$

$$\left\| \sum_{k=0}^{K-1} \Phi_{N,k}^{vv} \mathbf{u}_k + \mathbf{v}_0^N - \mathbf{v}_{N,\text{ref}} \right\|_2 \leq \epsilon_v. \quad (11b)$$

2) *Stable Subspace*: An alternative terminal constraint set is considered by making use of the stable subspace of the baseline NRHO. Specifically, the steered state is constrained to lie inside the conical combination of all stable basis vectors \mathbf{y}_i^s for $i = 0, \dots, S-1$. The corresponding set $\mathcal{X}_{\text{stb}}(t_N)$ is given by

$$\mathcal{X}_{\text{stb}}(t_N) = \left\{ \mathbf{x} \in \mathcal{X}_{\text{ell}}(t_N) : \mathbf{x} \in \mathbf{x}_{N,\text{ref}} \pm \sum_i \alpha_i \mathbf{y}_i^s \right\}. \quad (12)$$

where α_i are non-negative scalars. The set $\mathcal{X}_{\text{stb}}(t_N)$ can be implemented by enforcing, in addition to conditions (11), the following linear constraints

$$\mathbf{x}_0^N + \sum_{k=0}^{K-1} \begin{bmatrix} \Phi_{N,k}^{rv} \\ \Phi_{N,k}^{vv} \end{bmatrix} \mathbf{u}_k = \mathbf{x}_{N,\text{ref}} \pm \sum_{i=0}^{S-1} \alpha_i \mathbf{y}_i^s, \quad (13a)$$

$$\alpha_i \geq 0, \quad \forall i = 0, \dots, S-1, \quad (13b)$$

where $\mathbf{y}_i \in \mathbb{R}^6$ denote the i^{th} stable direction on the baseline at time t_N , and α_i for $i = 0, \dots, S-1$ are introduced as additional variables to scale along each stable direction.

C. Sequential Linearization Scheme

While the STM yields a reasonably reliable prediction of small perturbations over time, the nonlinearity of the dynamics is sufficiently high that a sequential linearization scheme has been previously found to improve the recursive convergence of SK algorithms [7], [18].

Problem (7) is recast as an SOCP by introducing slack variables for the 2-norm of \mathbf{u}_k for $k = 0, \dots, K-1$ in the objective (7a), replacing (7b) by either the SOC constraints (11) or both the SOC constraints (11) and the linear constraints (13), and using definition (9) for \mathcal{U} in constraint (7c).

At each iteration, \mathbf{x}_0^N , $\Phi_{N,k}^{rv}$ and $\Phi_{N,k}^{vv}$ are updated by incorporating controls computed from the previous iteration. Let $\mathbf{u}_0^{(i)}, \dots, \mathbf{u}_{K-1}^{(i)}$ denote the solution to problem (7) at the i^{th} iteration. On the next iteration, \mathbf{x}_0^N is obtained by

$$\mathbf{x}_0^N = \begin{bmatrix} \mathbf{r}_0^N \\ \mathbf{v}_0^N \end{bmatrix} = \mathbf{F}_u[\mathbf{x}(t), \mathbf{u}_{0,\text{prev}}^{(i)}, \dots, \mathbf{u}_{K-1,\text{prev}}^{(i)}, t], \quad (14)$$

instead of equation (8); in (14), $\mathbf{u}_{k,\text{prev}}^{(i)}$ is the cumulative k^{th} control given by

$$\mathbf{u}_k^{(i)} = \begin{cases} \mathbf{0}_{3 \times 1}, & i = 0, \\ \sum_{j=0}^{i-1} \mathbf{u}_{k,\text{prev}}^{(j)}, & i > 0. \end{cases} \quad (15)$$

Furthermore, $\Phi_{N,k}^{rv}$ and $\Phi_{N,k}^{vv}$ are constructed by linearizing the nonlinear flow around (14).

At time t_0 , the SKMPC requires as input the current state $\mathbf{x}_0 = \hat{\mathbf{x}}(t_0)$, targeted time t_N , the definition of the terminal constraint set $\mathcal{X}(t_N)$, admissible control set \mathcal{U} , and the maximum number of iterations for linearization M . Once the SKMPC solves problem (7), a sequence of controls $[\mathbf{u}_0, \dots, \mathbf{u}_{K-1}]$, each spaced one revolution apart according to condition (6), is obtained. The spacecraft executes \mathbf{u}_0 at time t_0 , and the spacecraft state is propagated until time t_1 ; at this time, problem (7) is solved again with updated time indices, sliding the targeting horizon t_N by one revolution, and a new sequence of controls is obtained.

IV. EXPERIMENT SETUP

The SKMPC is tested on a realistic scenario, recursively solving the SKMPC for an extended number of revolutions spanning multiple years, subject to error realizations drawn from predefined distributions. Each time the spacecraft arrives at $\theta(t) = 200^\circ$, we denote t as t_0 , and the SKMPC is invoked using a control horizon defined by (6) with $\theta_{\text{man}} = 200^\circ$.

A. Error Models

We assume realistic error models that exist in the SK operation of a spacecraft on an NRHO [2], consisting of: dynamics error, realized through random relative variation of A/m and C_r in the SRP term; reaction wheel desaturation error, realized by appending random impulses at four locations along the orbit in each revolution; navigation error, realized by appending noise on top of the true state; and maneuver execution error, realized by corrupting the maneuver with the Gates model [19]. The errors are implemented according to the recursive simulation setup in [7], with error values summarized in Table I; these values are taken to be corresponding to the assumed levels of uncertainties for the Gateway, provided in [2].

TABLE I: Error parameters

Error parameter	Value
SRP relative A/m 3- σ , %	30
SRP relative C_r 3- σ , %	15
Desaturation velocity perturbation 3- σ , cm/s	1.0
Desaturation location true anomaly, deg	340, 350, 10, 190
Navigation error position 3- σ , km	1.5
Navigation error velocity 3- σ , cm/s	0.8
Maneuver relative magnitude error 3- σ , %	1.5
Maneuver absolute magnitude error 3- σ , mm/s	1.42
Maneuver execution direction error 3- σ , deg	1.0

B. Control Trigger Condition

At each apolune, the need for an SK maneuver is determined by checking if the unsteered state predicted until time t_N lies within an ellipsoid about the baseline with radii $\epsilon_{r,\text{trig}}$ in position components and $\epsilon_{v,\text{trig}}$ in velocity components

$$\|\mathbf{r}_0^N - \mathbf{r}_{N,\text{ref}}\|_2 \leq \epsilon_{r,\text{trig}}, \quad \|\mathbf{v}_0^N - \mathbf{v}_{N,\text{ref}}\|_2 \leq \epsilon_{v,\text{trig}}. \quad (16)$$

Note that $\epsilon_{r,\text{trig}}$ and $\epsilon_{v,\text{trig}}$ do not need to be the same as the tolerances ϵ_r and ϵ_v used within the definition of the terminal constraints (11). In fact, choosing $\epsilon_{r/v} < \epsilon_{r/v,\text{trig}}$

builds hysteresis into the control scheme, thereby making it more robust against uncertainties.

V. NUMERICAL RESULTS

Controller parameters are given in Table II. Specifically, two controllers are considered: configuration A uses the stable subspace-based terminal set, while configuration B uses the simpler ellipsoid-based terminal set. We note that configuration B is expected to outperform A, as the smaller targeted set is expected to require larger controls, while the contracting behavior of the stable subspace is attenuated by the existence of noise.

For both controllers, the prediction horizon N has been tuned after preliminary testing to result in no failed scenarios for 100 Monte Carlo runs. Each run consists of 600 revolutions, which corresponds to 10.8 years on the NRHO. The choice of N is impacted by $\kappa(\Phi_{N,0})$ and by the various errors associated with the operation of the spacecraft. Note also that configuration A necessitates a smaller N as predicting the stable modes \mathbf{y}_i^s is more susceptible to errors than predicting the final state \mathbf{x}_0^N .

The dynamics is integrated using the explicit embedded Runge-Kutta Prince-Dormand (8,9) method from the GNU Scientific Library [20]. The SKMPC takes an average of 1.76 sec to solve on a single Intel i7-12700 CPU; the majority of the computational effort comes from propagating and constructing the STMs in (7b).

TABLE II: SKMPC configurations and parameters

Controller configuration	A	B
Terminal set $\mathcal{X}(t_N)$	Stable subspace	Ellipsoid
Control horizon K	2	2
Prediction horizon N	4	7
$\epsilon_{r,\text{trig}} / \epsilon_r$, km	100 / 25	100 / 25
$\epsilon_{v,\text{trig}} / \epsilon_v$, m/s	20 / 5	20 / 5

TABLE III: Delta-V cost statistics

Controller configuration	A	B
Per maneuver mean, cm/s	5.54	2.75
Yearly mean, cm/s	308.75	153.06
Yearly standard deviation, cm/s	17.95	8.01
Yearly 95 th percentile, cm/s	336.72	167.96

A. Choice of Terminal Constraint Set

Performances achieved by configurations A and B are summarized in Table III. Using the stable subspace \mathcal{X} requires an overall higher cost; with the chosen parameters, the SK cost is found to be approximately double that of the configuration using the ellipsoidal \mathcal{X} .

To gain further insight into the difference in performance between configuration A and B, Figure 2 shows the distribution of $u_0 = \|\mathbf{u}_0\|_2$ and $u_1 = \|\mathbf{u}_1\|_2$ from solutions of the SKMPC across 600 revolutions from a single Monte Carlo run. There is a stark difference between configurations A and B in terms of the reliance on the unimplemented second maneuver u_1 ; using the stable subspace \mathcal{X} is found to result in u_0 and u_1 being of similar magnitude and specifically

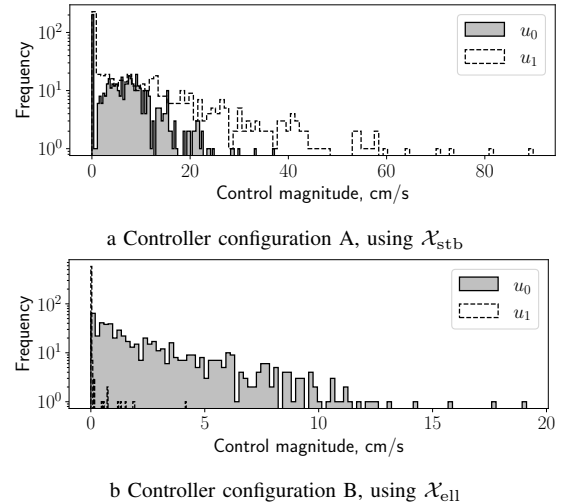


Fig. 2: Maneuver magnitudes from SKMPC solution over a single Monte Carlo run of 600 revolutions

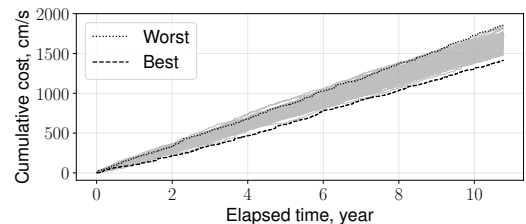


Fig. 3: Cumulative cost history using \mathcal{X}_{ell}

$u_1 > u_0$ in many cases, whereas using the ellipsoidal \mathcal{X} results in $u_0 > u_1$, with negligible u_1 in most cases. The higher reliance of the controller on the unused second maneuver results in poorer closed-loop performance.

B. Long-Term Performance

We analyze the performance of SKMPC with configuration B in closer detail to evaluate its efficacy as an SK method for the NRHO in comparison to state-of-the-art approaches proposed in the literature. Hereafter, all figures correspond to results using configuration B with the ellipsoidal $\mathcal{X}(t_N)$.

First, focusing on the cost performance of the controller, Figures 3 and 4 show the cumulative cost over 600 revolutions and the per-maneuver cost over the first 100 revolutions, respectively. The black trace in Figure 4 shows a typical Monte Carlo realization. The SKMPC results in a mean yearly cost of 153 cm/s, with a standard deviation of 8 cm/s.

For reference, with the x -axis crossing control, [2] report a mean yearly cost of 134 cm/s with a minimum of 120 cm/s and a maximum of 160 cm/s. The SKMPC's mean annual cost is comparable, with a higher average by about 20 cm/s, corresponding to a 15% per year increase.

We also focus on the tracking capability of the SKMPC; Figure 5a shows the deviation in perilune passage epoch between the controlled path and the baseline, and Figure 5b shows the corresponding deviation in perilune state. At perilune, where the spacecraft travels the fastest along the

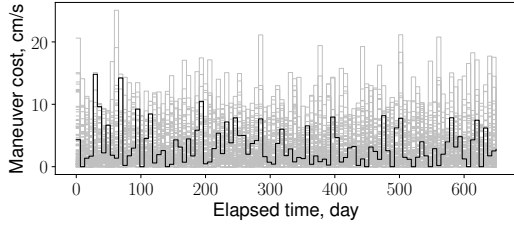


Fig. 4: Cost history during 100 revolutions using \mathcal{X}_{ell}

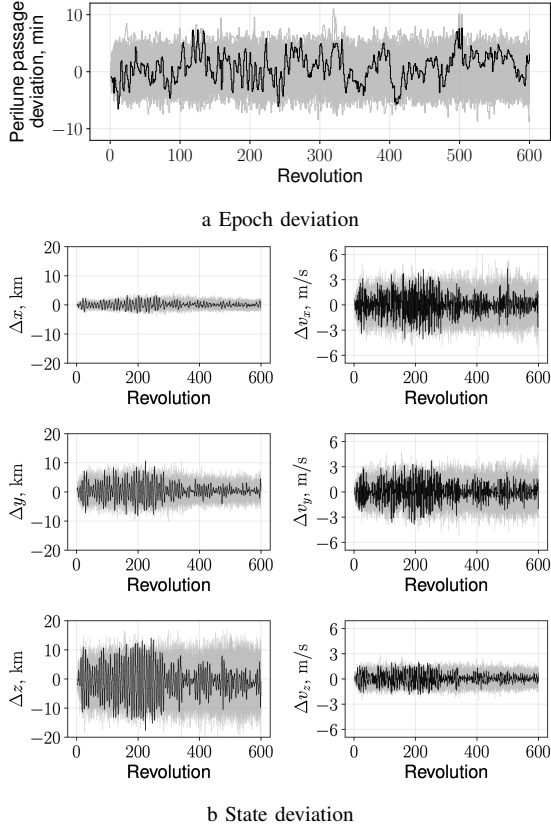


Fig. 5: Deviations at perilune passage using \mathcal{X}_{ell}

NRHO, the SKMPC tracks the baseline path to within about 20 km in position, 5 m/s in velocity, and 10 min in time. This tracking performance constitutes a significant improvement from the Gateway’s planned SK controller, reported by [2] to achieve perilune deviations of up to 80 km in position and 48 min in time. Overall, at the expense of a 15% control cost increase, the SKMPC achieves a much tighter perilune passage without requiring any ad-hoc augmentations necessitated by methods such as x -axis crossing control [2].

VI. CONCLUSION

We proposed a tracking MPC for the station-keeping problem on the NRHO. This SKMPC leverages multiple maneuvers within its control horizon to have sufficient degrees of freedom for full-state tracking. Meanwhile, by placing each maneuver in the control horizon one revolution apart, the proposed SKMPC can be used as a single maneuver-per-revolution scheme, a common operational requirement

in space missions on the NRHO to simplify the spacecraft’s operation. The SKMPC achieves cumulative maneuver costs comparable to state-of-the-art SK approaches proposed in the astrodynamics literature, while resulting in a tighter tracking of the reference orbit in both space and phase.

ACKNOWLEDGMENT

The authors thank Samet Uzun for helpful discussions.

REFERENCES

- [1] D. E. Lee, “Gateway Destination Orbit Model: A Continuous 15 Year NRHO Reference Trajectory,” NASA, Tech. Rep., 2019.
- [2] D. C. Davis, S. T. Scheuerle, D. A. Williams, F. S. Miguel, E. M. Zimovan-Spreen, and K. C. Howell, “Orbit Maintenance Burn Details for Spacecraft in a Near Rectilinear Halo Orbit,” in *AAS/AIAA Astrodynamics Specialists Conference*, 2022.
- [3] D. Guzzetti, E. M. Zimovan, K. C. Howell, and D. C. Davis, “Stationkeeping Analysis for Spacecraft in Lunar Near Rectilinear Halo Orbits,” in *AAS/AIAA Space Flight Mechanics Meeting*, 2017.
- [4] B. Cheetham, T. Gardner, A. Forsman, E. Kayser, and M. Clarkson, “CAPSTONE: A Unique CubeSat Platform for a Navigation Demonstration in Cislunar Space,” in *ASCEND 2022*. Reston, Virginia: American Institute of Aeronautics and Astronautics, 2022, pp. 1–10.
- [5] D. A. P. Williams, K. C. Howell, and D. C. Davis, “A Comparison of Station-Keeping Strategies for Halo Orbits,” in *AAS/AIAA Astrodynamics Specialist Conference*, vol. 231, 2023, pp. 1–20.
- [6] S. Baskar, E. W. Kayser, M. Popplewell, T. M. Bolliger, and L. Fahay, “Stationkeeping for transition region earth-moon halo orbits,” in *AAS/AIAA Astrodynamics Specialist Conference*, 2024.
- [7] Y. Shimane, K. Ho, and A. Weiss, “Optimization-Based Phase-Constrained Station-Keeping Control on Libration Point Orbit,” in *AAS/AIAA Astrodynamics Specialists Conference*, 2024, pp. 1–19.
- [8] M. Shirobokov, S. Trofimov, and M. Ovchinnikov, “Survey of station-keeping techniques for libration point orbits,” *Journal of Guidance, Control, and Dynamics*, vol. 40, no. 5, pp. 1085–1105, 2017.
- [9] D. Angeli, “Economic Model Predictive Control,” in *Encyclopedia of Systems and Control*, J. Baillieul and T. Samad, Eds. London: Springer London, 2015.
- [10] U. V. Kalabic, A. Weiss, S. Di Cairano, and I. V. Kolmanovskiy, “Station-keeping and momentum-management on halo orbits around L2 : Linear-quadratic feedback and model predictive control approaches,” in *AAS/AIAA Space Flight Mech. Meeting*, 2015.
- [11] G. Misra, H. Peng, and X. Bai, “Halo orbit station-keeping using nonlinear MPC and polynomial optimization,” in *AAS/AIAA Space Flight Mech. Meeting*, 2018.
- [12] P. Elango, S. Di Cairano, U. Kalabic, and A. Weiss, “Local Eigenmotion Control for Near Rectilinear Halo Orbits,” in *Proceedings of the American Control Conference*, vol. 2022-June, 2022, pp. 1822–1827.
- [13] R. Padhi, A. Banerjee, S. Mathavaraj, and V. Sriani, “Computational Guidance Using Model Predictive Static Programming for Challenging Space Missions: An Introductory Tutorial with Example Scenarios,” *IEEE Control Systems*, vol. 44, no. 2, pp. 55–80, 2024.
- [14] W. McClain and D. Vallado, *Fundamentals of Astrodynamics and Applications*, ser. Space Technology Library. Springer Netherlands, 2001.
- [15] C. Acton, N. Bachman, B. Semenov, and E. Wright, “A look towards the future in the handling of space science mission geometry,” *Planetary and Space Science*, vol. 150, no. January 2017, pp. 9–12, 2018.
- [16] E. M. Zimovan-Spreen, K. C. Howell, and D. C. Davis, “Dynamical Structures Nearby NRHOs with Applications to Transfer Design in Cislunar Space,” *Journal of the Astronautical Sciences*, vol. 69, no. 3, pp. 718–744, jun 2022.
- [17] K. Rivera Lopez and M. Holzinger, “Statistical Analysis of Optimal Stationkeeping Location and Coast Duration Using Stretching Directions,” *Journal of the Astronautical Sciences*, vol. 71, no. 1, feb 2024.
- [18] P. Elango, S. Di Cairano, K. Berntorp, and A. Weiss, “Sequential linearization-based station keeping with optical navigation for NRHO,” in *AAS/AIAA Astrodynamics Specialist Conference*, 2022.
- [19] C. R. Gates, “A Simplified Model of Midcourse Maneuver Execution Errors,” Jet Propulsion Laboratory, Tech. Rep., 1963.
- [20] B. Gough, *GNU scientific library reference manual*. Network Theory Ltd., 2009.